Neutral molecular beam formation or deceleration induced by optical lattices

M.N. Shneider

Princeton University, Princeton, NJ 08544

Abstract. A periodic optical dipole potential is created by the interaction of a polarizable particle with the field of an optical interference pattern (optical lattice) formed by counter propagating non-dissipative laser fields. The analysis of motion of trapped and untrapped particles, combined with the direct numerical simulation of the 1D non-stationary Boltzmann equation, demonstrates that atoms and molecules can be accelerated in chirped pulsed optical lattices from room temperature level to velocities in 10 to 100 km/s range over distances of hundreds of microns. A deceleration scheme that uses non-dissipative optical forces to slow molecules by decelerating the optical lattice from an initial velocity equal to that of a supersonic plume is also considered. The deceleration scheme is used in recent experiments performed by Dr. Peter Barker's group at Heriot-Watt University, UK. A number of other possible applications of optical lattice – neutral gas interactions are mentioned briefly.

Keywords: Optical lattice, non-resonant laser/gas interactions, molecular acceleration/deceleration
PACS: 51.10.+y, 51.90.+r

INTRODUCTION

In this paper, we present a brief overview of recent experimental and theoretical studies of the interaction of neutral gases with optical lattices produced by non-resonant laser radiation.

Small gas density perturbations produced by relatively weak intensity laser beams (when the optical lattice potential well depth $\ll$ kT) can be used for powerful nonintrusive diagnostics based on Coherent Rayleigh [1, 2] and Coherent Raleigh-Brillouin scattering in gases [3, 4, 5]. In this case, a probe laser beam was coherently scattered from the density perturbation waves induced by an optical lattice. The line shape of the scattered signal was modeled using the kinetic theory. In the high intensity regime where the optical lattice potential is comparable to the thermal energy of gas particles, a Coherent Raleigh scattering (low density limiting case of the Coherent Raleigh-Brillouin scattering) line shape narrowing phenomenon was predicted [6] and recently has been observed experimentally [2].

The transport and dynamics of ultra-cold atoms in shallow (mK) periodic optical potentials called optical lattices have been widely studied[7, 8] and, more recently, deceleration and acceleration of molecular and atomic species traveling in a supersonic beam has been demonstrated using deep (100 K) optical lattices [9, 10].

Recently, it has been shown [11, 12] that when an optical periodic potential created by a light field affects neutral atoms or molecules with a finite polarizability, in the collisionless regime these particles undergo a process similar to Landau damping. This process was called optical Landau damping because, in a sense, this process is analogous to the collisionless Landau damping observed in plasmas [13, 14]. In the optical Landau damping, the dissipation of the optical wave is transformed into particle motion via the dipole force. Note that in the laser induced drift (LID) of atomic and molecular species, which does not employ the dipole force [15], the drift results from a flux imbalance created by the difference in collisional cross sections between optically induced excited states and the ground state of particular gas species. It occurs only when the resonant species is in a buffer gas [15] or in a narrow capillary [16] where a buffer gas is substituted by collisions with capillary walls. For LID, velocities in the cm/s range have been achieved. In contrast to LID, molecular transport induced by weak periodic optical dipole forces may be achieved in single-species gases in collisionless and low collisional [11, 12] and highly collisional regimes [17].

Linear acceleration within the time varying electric field of an accelerated optical traveling wave has been proposed as a means to accelerate atoms to high velocity [18, 19] and, more recently, a molecular acceleration has been proposed [20, 21]. Linear acceleration using optical fields is attractive because extremely large dipole forces can be produced by the high electric field gradients that can be created within an optical traveling wave. The electrodeless electric field gradient produced by a focused laser beam can be orders of magnitude greater than electrostatic gradients, allowing acceleration of not only polar but also polarizable molecules and atoms. This concept has already been demonstrated

with acceleration of ultracold atoms up to velocities in the m/s range using very weak optical lattices [22, 23]. A one dimensional optical lattice is created by two counterpropagating laser beams, and acceleration of the lattice is achieved by changing the frequency of the counter propagating fields (chirping) with respect to time.

Synchronous acceleration of charged particles to energies in excess of 100 GeV can be achieved using electrostatic and Lorentz forces, and accelerated neutral atomic beams can be created from ion beams by charge capture [24]. Gas dynamic methods that accelerate molecules to greater than 10 km/s (14.5 eV for N_2) [25] have been demonstrated, but to our knowledge no method has been proposed to accelerate neutral molecules above this energy range without a large fraction of the gas being thermally ionized and dissociated [26].

The interaction between high density gases and non-resonant laser radiation produced by deep optical lattices was also investigated. Each of the laser beams creating the lattice was considered to be non-resonant with internal degrees of freedom of molecules, which has resulted in a localized gas-lattice interaction only in the lattice region. Collisional momentum and energy transfer from an optical lattice to gas molecules was examined analytically and numerically [17, 27, 28]. The possibility of non-intrusive creation of localized molecular beams in unbounded high density gases was shown for the first time [17, 27]. It has also been shown that, for a gas flow in a capillary, a pressure differential along the capillary is produced due to gas-lattice interaction, which can be used to separate gas species based on their polarizability [17] .

The non-resonant interaction of gas molecules with the optical lattice potential was also studied with application to rocket propulsion [29]. The principal driving force for the non-resonant laser propulsion at high densities is the energy and momentum deposition from optical lattice to gas. Analytical model has been developed to qualitatively characterize this deposition; the results of the model are in good agreement with the DSMC predictions [17, 27]. The non-resonant acceleration of molecules to velocities of 10 km/s and higher in a chirped frequency optical lattice was suggested for use in the proposed low-density propulsion device. Stagnation pressures from 0.01 to 1 torr were investigated, and a seven-fold increase in the specific impulse was obtained. The shown ability of the optical lattice to accelerate molecular beams to extremely high velocities in weakly collisional regime without ionization and dissociation of molecules may be used not only in propulsion, but also in various material processing devices.

Although there is a number of possible applications of the optical lattice – gas interactions, the main topic of this paper is neutral molecular beam formation and closely related reverse problem of molecular beam deceleration. Note, the maximum laser intensity that can be used to accelerate neutral particles, both atoms and molecules, is limited by ionization [30]. In all numerical simulations presented in this paper, the laser intensity is below the ionization saturation intensity of organic molecules measured in reference [30].

OPTICAL LATTICES

A periodic optical dipole potential is created by the interaction between a polarizable particle and the field of an optical interference pattern created by counter propagating laser fields with wave vectors $\overrightarrow{k}_1$ and $\overrightarrow{k}_2$ (Fig.1). The phase velocity of the pattern, and therefore the potential, is given by $\xi = \Omega/q$, where $q = \left|\overrightarrow{k}_1 - \overrightarrow{k}_2\right|$is the wavenumber, and $\Omega = \omega_1 - \omega_2$. A moving optical lattice can conceptually be created by a single laser and a mirror when the laser radiation with k_1, ω_1 reflects from the mirror moving with the velocity v_m where $\overrightarrow{v_m} \parallel \overrightarrow{k_1}$. Due to the Doppler effect, the reflected light in the laboratory frame has a frequency $\omega_2 \approx \omega_1(1-2v_m/c)$,when $|v_m|/c \ll 1$. The corresponding wave number of the reflected counter beam is $k_2 = k_1(1-2v_m/c)$ and the interaction of the primary laser and the reflected beams results in the traveling interference pattern with the phase velocity $\varsigma = \frac{\omega_1-\omega_2}{k_2+k_1} = \frac{2\omega_1 v_m/c}{k_1(1+1-2v_m/c)}$. In the non-relativistic limit, $v_m/c << 1$,the phase velocity of the optical lattice traveling wave is equal to the velocity of the mirror, $\varsigma = v_m$. In practice, a moving lattice is created by a frequency difference between the counterpropagating fields.

For molecules that are far detuned from resonance the force on the molecules within a lattice is given by the quasi-electrostatic approximation given by [31, 32]

$$\overrightarrow{F}(x,t) = \frac{1}{2}\alpha\nabla E(x,t)^2 \tag{1}$$

where α is the static polarizability and $E(z,t)$ is the optical electric field. For infrared fields in the 1 μm range, the first single photon resonance of many molecules is in the UV and VUV region. At high intensities (10^{12} W/cm^2),

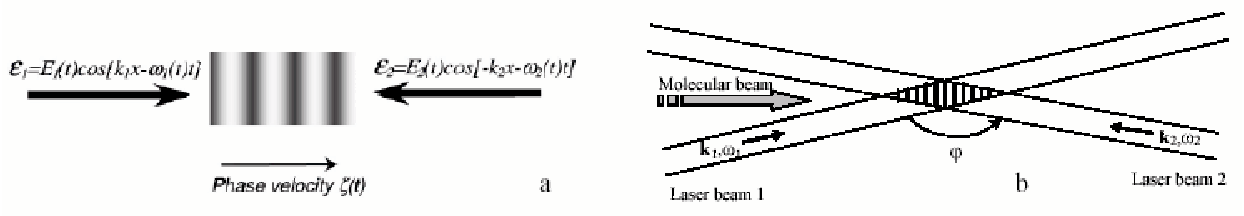

FIGURE 1. The creation of an optical lattice by two counterpropagating optical fields for transport of molecules and atoms. (a) - idealization; (b) - practical beam arrangement with the angle $\varphi \lesssim 180^0$.

pendular states can be created when the pulse duration is greater than the rotational period [34]. In this process, the molecule vibrates around the polarization direction of the optical field effectively aligning the molecule with the field. This process increases the optical force since it leads to a higher effective polarizability when compared to the static polarizability. The polarizability of a molecule that is not aligned within the field is given by $\alpha = (\alpha_{\|} + 2\alpha_{\perp})/3$, where $\alpha_{\|}$ and $\alpha_{\perp}$ are the parallel and perpendicular components of the static polarizability with respect to the molecular axis [33]. This expression is a lower limit to the force because, in an intense field, molecular alignment of the molecule with the field has been shown to occur when the pulse duration is greater than inverse of the rotational rate. At high intensities (10^{12} W/cm^2), pendular states can be created when the pulse duration is greater than the rotational period [34]. In this process, the molecule vibrates around the polarization direction of the optical field effectively aligning the molecule with the field [35, 36].

OPTICAL MICROLINEAR ACCELERATOR

In contrast to acceleration of ultracold atoms in weak lattices[22, 23], we have studied the acceleration of polarizable gas particles, such as molecules and atoms at much higher temperatures (5-300 K), to velocities in the 10 to 100 km/s range by application of large lattice potentials created by pulsed lasers. Our work follows on from the original work of Kazantsev [18, 19], and investigates the motion of trapped and untrapped particles in the velocity phase space of the accelerated optical dipole potential. We study the dynamics of the accelerating ensemble of polarizable particles under the influence of large dipole or stark forces, and predict the velocity distribution function of both trapped and untrapped particles [37].

We consider an accelerating optical lattice that is formed by two almost counterpropagating fields, as shown in Figure 1. The lattice traps and transports the trapped particles to the desired velocity by acceleration. The slowly varying interference term between the two counterpropagating fields that leads to the acceleration is given by $E(x,t)^2 = E_1(t)E_2(t)\cos(qx-\beta t^2)$, where $\beta = \frac{d\Omega(t)}{dt}$ is the frequency chirp due to the time dependent frequency difference between each of the fields where $\Omega(t) = \omega_1(t) - \omega_2(t)$. We require that $\Omega(t) << \omega_1(t), \omega_2(t)$, and therefore that q is approximately constant over the chirped frequency range. In Figure 1, the instantaneous phase velocity indicates for a positive chirp and the phase velocity, $\zeta(t)$, of the lattice is given by: $\zeta(t) = \frac{2\beta t}{q}$.This is also the average velocity of a particle that is trapped and accelerated by the lattice. We consider acceleration of ensembles of 'hot' particles that are initially at thermal equilibrium near room temperature, and do not consider the quantized motion of the particles. The equation of motion for a particle that is perturbed by the periodic potential of the optical lattice is given by [37] $\frac{d^2x}{dt^2} = \frac{1}{2}\frac{\alpha q E_1(t)E_2(t)}{m}\sin(qx-\beta t^2)$, where m is the mass of the accelerated particle. In a reference frame that accelerates with the optical lattice, this equation in non-dimensional units, is now given by: $\frac{d^2\theta}{dT^2} = -aq\sin\theta - 2$,where $\theta = X - T^2$ is the phase of the particle with respect to the accelerated frame, and $T = \sqrt{\beta}t$ and $X = qx$ are the non-dimensional temporal and spatial variables respectively. The maximum force per unit mass supplied by the optical lattice is given by $a = \frac{1}{2}\frac{\alpha q E_1(t)E_2(t)}{m}$, and for most of this paper we assume that the electric field amplitudes are equal and constant in time, $E_1(t), E_2(t) = E_1, E_2$. We have assumed that the optical fields are sufficiently far detuned from resonance so that the force is harmonic [38].

To understand the motion of both trapped and untrapped particles within the lattice, it is instructive to investigate the trajectory of particles in the velocity phase space, $[\eta,\ \theta]$, from the system, given by: $\frac{d\eta}{dT} = -\frac{aq}{\beta}\sin\theta - 2$ and

$\frac{d\theta}{dT} = \eta$.The critical points correspond to $\sin\theta = -\frac{2\beta}{aq}$, and $\eta = 0$. A linear stability analysis around the critical points indicate that the family of points $[\theta,\eta] = \left[2n\pi - \sin^{-1}\psi, 0\right]$ are stable equilibrium points, where n is an integer and $\psi = \frac{2\beta}{aq}$. The points $[\theta,\eta] = \left[(2n-1)\pi + \sin^{-1}\psi, 0\right]$ are unstable equilibrium or saddle points.

For a lattice with a stable equilibrium point, $\sin\theta = -\psi$ and therefore: $\psi = \left|\frac{2\beta}{aq}\right| < 1$ is the condition for a particle to be trapped and accelerated by the lattice [37]. This condition implies that the chirp, β, must be less than $\frac{aq}{2}$, and confirms the intuitive result that the acceleration of the lattice, $a_L = \frac{2\beta}{q}$, must be less than a, the maximum force per unit mass supplied by the gradient of the lattice potential. The depth of the potential well in each case is determined by the difference in potential height between a saddle point and its closest equilibrium point. The potential well depth, ΔU, is given by: $\Delta U = \frac{ma}{q}\left[2\cos(\sin^{-1}\psi) - \psi(\pi - 2\sin^{-1}\psi)\right]$.It can be seen that no potential well exists for case $\psi \geq 1$, because either the chirp is too high, or the force per unit mass supplied by the lattice is not sufficient to trap particles. The maximum well depth is given by $\Delta U_{\max} = \frac{2ma}{q}$ when $\psi = 0$ which corresponds to the case with no chirp or acceleration. In the accelerated frame, any particle that is initially trapped in the potential well will remain in the well and oscillate about the stable critical point, $[\theta,\eta] = \left[2n\pi - \sin^{-1}\psi, 0\right]$, with a characteristic frequency that depends on its initial phase and velocity. Acceleration without oscillation occurs only for particles initially at this critical point. The maximum velocity half-spread of the trapped and accelerated particles is given by: $\Delta v = \sqrt{2\Delta U/m}$,which determines the maximum velocity deviation that a trapped particle can attain in its oscillation around the stable equilibrium point. For a lattice with $\psi = 0.59$, $a = 2.14\times10^{12}$ m/s^2, $q = 1.57\times10^{7}$ m^{-1}, where the electric field for each beam is $E_1 = E_2 = 5\times10^{9}$ V/m, the potential well depth of $\Delta U \approx 133$ K corresponds to a velocity spread of 735 m/s.

Acceleration of an ensembles of particles

The evolution of particles that are distributed over a range of velocities, and over all phases, can be conveniently calculated from the collisionless Boltzmann equation. To calculate the velocity distribution we assume, for simplicity, a periodic potential with infinite length. This condition elucidates the essential physics and allows the use of the cyclic boundary condition $f(-L/2,v,t) = f(L/2,v,t)$, where $L = 2\lambda$, and where $\lambda = 4\pi/q$ for counterpropagating beams. The Boltzmann equation was also subject to the boundary conditions $f(x, v\to\pm\infty, t) = 0$ and was numerically integrated with an initial condition $f(x,v,t=0) = f_0(v,T_0)$, where $f_0(v,T_0)$ is the equilibrium Maxwell distribution at gas temperature T_0.

Figure 3 shows the evolution in time of an ensemble of thermally distributed CH_4 molecules, that are initially at temperature $T_0 = 300$ K, and are perturbed by an accelerating optical lattice [37]. The top hat temporal intensity profile is chosen so that the results can be compared with the velocity-phase diagram of Figure 2,a**.** The evolution of the initial Maxwell distribution function is calculated by integration of the Boltzmann equation, as discussed above. The distribution function is averaged over the spatial period of the lattice at each time. The top hat profile has the ratio $\psi = 0.59$, which corresponds to a total laser intensity (both beams) of 6.5×10^{16} W/m^2(6.5×10^{12} W/cm^2), and a chirp of 1×10^{19} rad/s^2. We use the static polarizability of CH_4.

Approximately 30 % of the particles are trapped and accelerated at the phase velocity, reaching 10.2 km/s in the 8 ns duration of the calculation. The long tail between the largely unperturbed distribution at $v = 0$ m/s and the accelerated distribution is caused by molecules that are undergoing incomplete unstable orbits around the stable region in the phase space. After 2 ns, the number of particles in the accelerated distribution is approximately constant, indicating that the integration scheme is working correctly and that no particles are being numerically lost from the accelerated distribution. This accelerated distribution is almost Gaussian with a full width half maximum velocity spread that corresponds to a temperature in the accelerated frame of 41 K. It is emphasized that the initial temperature of the ensemble does not determine the energy spread of the accelerated distribution, only the fraction that will be accelerated. For comparison, Figure 3,b shows the evolution of the an ensemble of CH_4 molecules that are perturbed by a Gaussian temporal intensity profile with an initial lattice velocity of -5 km/s and the same chirp of $\beta = 1\times10^{19}$ rad/s^2. The full width half maximum (FWHM) intensity of this Gaussian profile is 6.5×10^{15} W/m^2, which is the same as the top hat profile intensity in Figure 3,a. As expected, the fraction of accelerated particles varies during the pulse because both ψ and the potential well depth ΔU vary during the acceleration period. In this case, at most 11 % of the particles are trapped and accelerated, compared to 30 % for the top hat profile. The width of the accelerated distribution decreases as particles are lost from the lattice because the intensity rolls off in the latter part of the pulse. The number of particles in the long tail behind the accelerated distribution increases as these particles are lost from the lattice. Because we

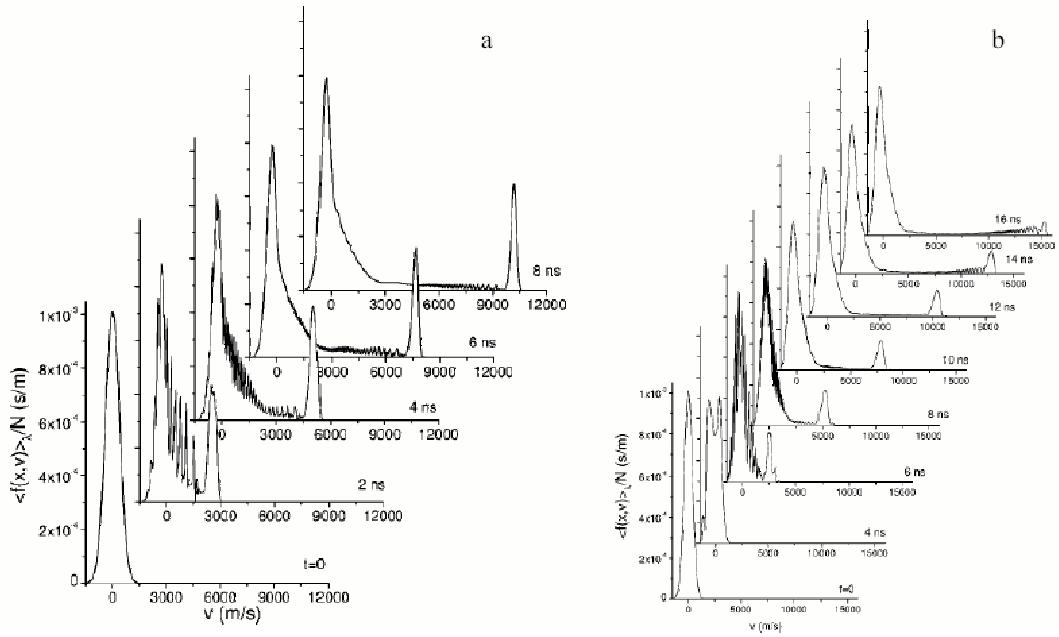

FIGURE 2. (a) The instantaneous velocity distribution function of CH4 molecules within an accelerating optical lattice in 2-ns time increments after the lattice is created. The distribution function was averaged over the spatial period of the lattice and ψ =0.59. (b) The instantaneous velocity distribution function of CH4 molecules within an accelerating optical lattice with a Gaussian temporal profile, in 2-ns time increments. The velocity distribution functions were averaged over the spatial period of the lattice at each time moment.

must start at a negative velocity, the final velocity that can be reached by starting at -5 km/s is approximately half that achieved by the top hat profile. These results indicate, that in a experiment, higher performance will be achieved for fields which can be rapidly switched on and off. The spatial variation of beam intensity must also be taken into account, since this will determine the number and spatial extent of the accelerated particles, as well as the variation in velocity across the beam. The spatial and temporal variation of the laser field will not change an essential physics of an acceleration process, but as shown above for the Gaussian temporal profile, they both must be considered to correctly model an experiment.

Collisional dynamics

To model the evolution of particles at higher pressures, when the collision time in a gas becomes on the order of the pulse duration, and the molecular collisions are important, the full integro-differential Boltzmann equation has to be solved. One of the most convenient and widely used approaches to the solution of the Boltzmann equation is the DSMC method. This method has been used in all presented computations. The principal computational tool used in this work is SMILE, an advanced code based on the DSMC method. Details on the tool may be found elsewhere.[39]

When molecular collision time becomes close to the pulse duration, the collisional relaxation causes a three-fold degradation of the trapped molecules peak. It is however remarkable that even at a pressure of 3 torr there is a significant number of molecules (about 3%) with velocities over 10 km/s. The collisions of trapped and untrapped molecules produce a significant number of molecules with velocities between 0 and 14 km/s. Note also that due to these high-energy collisions there are more molecules with large negative velocities at a pressure of 3 torr. At even higher gas pressures, 1 atm and higher, molecular collisions will result in rapid gas maxwellization during the pulse and efficient dissipation of laser energy over all molecules.

Note, that we have used the static polarizability to describe the force on polarizable particles because, for many molecules, the laser sources available are far from resonance. However, for many atoms and some molecules, the laser sources can be tuned closer to resonance, and the force per unit mass provided by the optical field can be increased

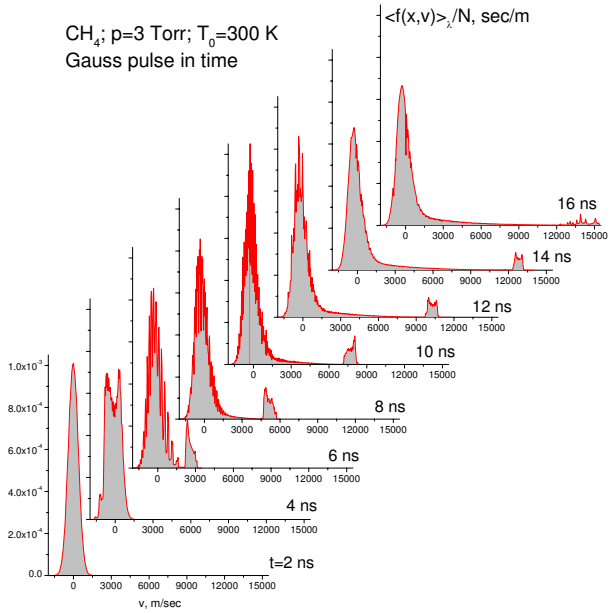

FIGURE 3. Distribution function of molecular velocities at different time moments for 3 torr.

by at least an order of magnitude over the static case [18]. In these cases, the number of particles that can be trapped and accelerated can be increased, or the number of particles can be held fixed while increasing the final velocity of the accelerated distribution by increasing the chirp.

SLOWING OF MOLECULES WITH A TRAVELING OPTICAL LATTICE

The reverse to acceleration process is a molecular beam deceleration. The creation of essential amount of the cold molecules in the sub-Kelvin temperature range is very important for many application: from precise spectroscopy and van der Waals interaction studies to cold chemistry. Recently, synchronous deceleration of dipolar molecules using time dependent stark forces has been demonstrated [40]. In this technique, polar molecules are trapped and decelerated in a stark potential created by an electro-static traveling wave produced by up to 68 electrode stages. This scheme was used to decelerate jet of dipolar molecules moving at supersonic speeds to near zero velocity. For the case of ND_3, a density of $10^6 cm^{-3}$ was decelerated to zero velocity in the laboratory frame and trapped electrostatically. As pointed out by the authors [40], this concept could also be used to accelerate dipolar molecules to high energy and velocity, in analogy to the synchronous acceleration in charged particle accelerators.

We suggested the creation of a cold ensemble of molecules by optical dipole or Stark deceleration [41]. This scheme is the optical analog of the successful electrostatic scheme which has been used to slow a range of dipolar molecules [40]. Although high intensity fields are required, we operate far from resonance, while maintaining the intensity well below a value where multiphoton ionization, tunneling ionization or dissociation would cause significant neutral molecule depletion. We previously explored the application of this general scheme for producing an accelerated ensemble of molecules or atoms. In the paper [41] we show that this scheme could be used to slow heavy polarizable molecules and presented results for I_2 as an example. Our deceleration scheme uses non-dissipative optical forces to transfer jet-cooled molecules in a supersonic expansion (10^{12} cm^{-3}) to zero velocity in the laboratory frame. To slow the molecules a decelerating optical lattice with an initial velocity equal to that of a supersonic gas is created. By chirping one of the two counterpropagating beams, the lattice velocity decelerates in time reducing the velocity of the trapped molecules. Analysis of the phase trajectories gives similar results as in the considered above accelerator case [37].

Recently, the deceleration scheme was realized for NO [9, 10] and C_6H_6 molecules [42]. Experimentally [10] the dynamics of cold (1.8 K) NO molecules initially traveling at 400m/s within a molecular beam, perturbed by an optical lattice with an average well depth of 22 K and 5.8-ns duration was measured. To probe the motion of the molecules after

the lattice was turned off, they were ionized using a resonantly enhanced multiphoton ionization (REMPI) scheme. The velocity of the ions, and thus the neutrals along the y axis, was determined by their time-of-flight in a mass spectrometer. Figure 4 shows plots of the measured velocity distribution of molecules in the lattice for a range of lattice velocities. Each plot is labelled with the lattice velocity relative to the molecular-beam velocity. Adjacent to the experimental plots are simulations of the velocity distribution for each lattice velocity. For comparison, the unperturbed velocity distribution functions are also shown. For lattice velocities less than the molecular-beam velocity (-79, -52, -26 m/s), a significant fraction of the probed molecules is decelerated, and conversely, for lattice velocities greater than the molecular-beam velocity (52, 26 m/s), molecules are accelerated, with approximately the same velocity spread as the initial unperturbed molecular beam. Our simulations, based on a solving of a 1D Boltzmann equation with the force term determined by the experimental laser pulse intensities, show all of the major features measured in the experiment.

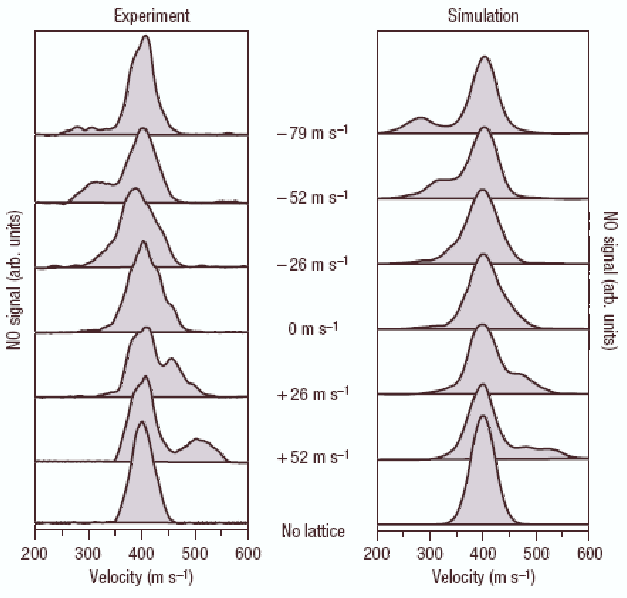

FIGURE 4. The velocity distribution function of NO molecules perturbed by the optical lattice. Lattice velocities with respect to the molecular-beam velocity of -79, -52, -26, 0, 26 and 52 m/s are shown. For comparison, simulations of the perturbed distribution function created by the different velocity lattices is shown alongside the experimental data.

CONCLUDING REMARKS

Microlinear acceleration by optical lattices may be used to produce neutral atomic and molecular beams with velocities in the 100 km/s range over distances of less than 1 mm. The beams have higher velocities and larger densities than those produced by pulsed molecular beams or other gas dynamic means. The final beam energy and the energy spread can be manipulated by laser fluence, frequency chirp, and pulse duration. Such a configurable, intense, and compact source of high-energy neutral particles may find application to collision studies, lithography, and atomic and molecular implantation or etching.

ACKNOWLEDGMENT

The author gratefully acknowledges Peter Barker and Sergey Gimelshein, co-authors of the work reviewed in this paper.

REFERENCES

1. J. Grinstead and P. F. Barker, Phys. Rev. Lett. **85**, 1222 (2000)
2. H. T. Bookey, A. I. Bishop, M. N. Shneider, P. F. Barker, J. Raman Spectrosc.,**37**, 655 (2006)
3. X.P. Pan, M.N. Shneider, R.B. Miles, Phys.Rev.Lett **89**, 183001 (2002)
4. X.P. Pan, M.N. Shneider, R.B. Miles, Phys.Rev.A **69**, 033814 (2004)
5. X.P. Pan, M.N. Shneider, R.B. Miles, Phys.Rev.A **71**, 045801 (2005)
6. M.N.Shneider, P.F.Barker, , X.P.Pan, R.B.Miles, Optics Communications, **239**, 205-211 (2004)
7. S.R. Wilkinson, C.F. Bharucha, M.C. Fisher, K.W. Madison, P.R. Morrow, Q. Niu, B. Sundaran, and M.G. Raizen, Nature **387**, 575 (1997).
8. D.A. Steck, W.H. Oskay, M.G. Raizen, Science **293**, 274 (2001).
9. Barker PF, Bishop AI, Fulton R, Shneider MN, Abs. of papers of the american chemical society 228: U244-U244 294-PHYS Part 2, AUG 22 (2004).
10. R.Fulton, A.I. Bishop, M.N.Shneider, P.F. Barker, Nature. Physics. **2**, 465 (2006)
11. M.N. Shneider, P.F. Barker, Proc. SPIE **5448**, 193 (2004)
12. M.N. Shneider and P.F. Barker, Phys. Rev. A. **71**, 053403 (2005)
13. L.D. Landau, Zh. Eksp. Teor. Fiz. **16**, 949 (1955)
14. B.B. Kadomtsev, Collective Phenomena in Plasmas, Pergamon Press; 1982
15. F. Kh. Gel'mukhanov, A.M. Shalagin, JETP Lett., **29**, 7111 (1979)
16. A.E.Bazelian, M.N.Kogan, DAN SSSR, **310** (1), 43 (1990)
17. M.N. Shneider, P.F. Barker, S.F. Gimelshein, J. Appl. Phys., **100** (2006)
18. A.P. Kazantsev, Sov. Phys. JETP, **36**, 861 (1973)
19. A.P. Kazantsev, Sov. Phys. JETP, **39**, 784 (1974)
20. P.B. Corkum, C. Ellert, M. Mehendale, P. Dietrich, S. Hankin, S. Aseyev, D. Rayner, D. Villeneuve, Faraday Discuss., **113**, 47 (1999)
21. H. Stapelfeldt, H. Sakai, E. Constant, P.B. Corkum, Phys. Rev. Lett. **79**, 2787 (1997)
22. K.W. Madison, C.F. Bharucha, P.R. Morrow, S.R. Wilkinson, Q. N. B. Sundaram, M.G. Raizen, Appl. Phys. B, **65**, 693 (1997)
23. E. Peik, M. Ben Dahan, I. Bouchoule, Y. Castin, C. Salomon, Appl. Phys. B, **65**, 685, (1997)
24. M.S. Livingston, J.P. Blewett, *Particle Accelerators,* (McGraw-Hill, New York, 1962)
25. A.J. Neely, R.J. Morgan, Aeronaut. J., **98**, 97 (1994)
26. R.B. Miles, G.L. Brown, W.R. Lempert, R. Yetter, G.J. Williams, S.M. Bogdanoff, D. Natelson, J.R. Guest, AIAA J., **33**, 1463 (1995)
27. M.N. Shneider, C. Ngalande, S.F. Gimelshein, AIAA paper 2006-0768
28. C.Ngalande, M.N. Shneider, S.F.Gimelshein, AIAA paper 2006-2900
29. M.N. Shneider, S.F. Gimelshein, P.F. Barker, J. Appl. Phys., **99,** 063102 (2006)
30. S.M. Hankin, D.M. Villeneuve, P. B. Corkum, D. M. Rayner, Phys. Rev. Lett., **84**, 5082 (2000)
31. R.W. Boyd, *Nonlinear Optics*, (Academic Press, Boston, 1992)
32. T. Takekoshi, J.R. Yeh, R.J. Knize, Opt. Comm. **114**, 421 (1995)
33. H. Sakai, A. Tarasevitch, J. Danilov, H. Stapelfeldt, R.W. Yip, C. Ellert, E. Constant, P.B. Corkum, Phys. Rev. A., **57**, 2794 (1998)
34. B. Friedrich, D. Herschbach, Phys. Rev. Lett. **74**, 4623 (1995)
35. H. Sakai, C. P. Safvan, J. J. Larsen, K. M. Hiligsoe, K. Hald, H. Stapelfeldt, J. Chem. Phys., **110**, 10235, (1999)
36. J. J. Larsen, H. Sakai, C. P. Safvan, I. Wendt-Larsen, H. Stapelfeldt, J.Chem. Phys., **111**, 7774 (1999)
37. P.F. Barker, M.N. Shneider, Phys. Rev. A. **64**, 033408 (2001)
38. H.J. Metcalf, P. van der Straten, *Laser cooling and trapping*, (Springer-Verlag, New York, 1999)
39. M.S. Ivanov, G.N. Markelov, S.F. Gimelshein, AIAA Paper 98-2669
40. H.L. Bethlem, G. Berden, F.M.H. Crompoets, R.T. Jongma, A.J.A. van Roij, G. Meijer, Nature **406**, 491 (2000)
41. P.F. Barker, M.N. Shneider, Phys. Rev. A. **65**, 065402 (2002)
42. R.Fulton, A.I. Bishop, M.N.Shneider, P.F. Barker, J.Phys.B, **39** (2006)